Non-specular ion reflection at quasiperpendicular collisionless shock front

Prachi Sharma [1],† and Michael Gedalin [1]

[1]Department of Physics, Ben Gurion University of the Negev, Beer-Sheva 8410501, Israel

The structure of a collisionless shock affects ion motion in the shock front and is affected by the formed ion distribution. In high-Mach-number shocks, a significant fraction of incident ions are reflected by the macroscopic electric and magnetic fields in the shock front. Ions are non-specularly reflected by the combined electric deceleration and magnetic deflection. Here, a first analytical description of the non-specular reflection is presented. The contribution of the increasing magnetic field is evaluated and shown to enhance reflection. The distribution of non-specularly reflected ions ahead of the ramp is calculated and their velocities at the re-entry to the shock are found numerically. Dependence on the angle between the shock normal and the upstream magnetic field vector is illustrated.

Keywords: astrophysical plasmas, plasma heating, space plasma physics

---

1. Introduction

Collisionless shocks are one of the most fundamental phenomena in space plasmas and among the most efficient accelerators of charged particles. Within the magnetohydrodynamical description, a fast shock is a discontinuity on which the plasma density, magnetic field, temperature jump and the flow speed drop (De Hoffmann & Teller 1950). Real collisionless shocks are of finite width with a rather complicated structure (Scudder *et al.* 1986). The latter is related to absence of collisions, which results in different responses of different populations of particles to the fields in the shock front. Over the past several decades, theoretical models, numerical simulations, *in situ* observations and laboratory experiments have all been used to understand the physics of collisionless shocks (see, e.g. Bell 1978; Kennel, Edmiston & Hada 1985; Stone & Tsurutani 1985; Sagdeev & Kennel 1991; Bykov *et al.* 2019, and references therein). Perri *et al.* (2022) review the latest advancements in particle acceleration, with a particular focus on shock acceleration.

The only place where the shock structure may be studied with *in situ* observations is the heliosphere. The shock structure depends on the angle θ_{Bn} between the shock normal and the upstream magnetic field vector (Bale *et al.* 2005; Burgess *et al.* 2005).

† Email address for correspondence: ps5739@gmail.com

Quasi-perpendicular shocks, $\theta_{Bn} > 45°$, have a well-developed structure of the magnetic field. Quasi-parallel shocks are believed to have a less regular shock front. However, this is not a rule and a quasi-perpendicular shock may look quasi-parallel or *vice versa*. See, e.g. the plots of the shocks in the Magnetospheric Multiscale database (Lalti *et al.* 2022). In what follows, we address those shocks which possess a well-defined magnetic structure: a narrow ramp with the steepest increase of the magnetic field and a wider overshoot in which the magnetic field reaches its maximum value.

Most high-resolution measurements have been done at the Earth bow shock. These measurements have shown that a part of incident ions may be reflected off the shock front and return to the upstream region just ahead of the shock transition, before either crossing the shock again toward downstream or escaping into the upstream region (Gosling *et al.* 1982; Sckopke *et al.* 1983, 1990; Goodrich *et al.* 2019). In low-Mach-number shocks, there are no, or almost no, reflected ions and the magnetic field profile is nearly monotonically increasing or has a small overshoot (Farris, Russell & Thomsen 1993; Balikhin *et al.* 2008). The overshoot is the region where the magnetic field is larger than it is in the uniform region well downstream of the shock. The overshoot arises due to the deceleration of the ion flow and drop of the ion pressure below the uniform downstream value (Ofman *et al.* 2009; Gedalin, Friedman & Balikhin 2015; Gedalin 2019*a*,*b*), while ion heating is due to the gyration of the directly transmitted ions (Gedalin 1997, 2021). With the increase of the Mach number the downstream magnetic field increases, which causes a stronger drop of the ion pressure and a larger overshoot (Mellott & Livesey 1987; Gedalin *et al.* 2023). In supercritical shocks (the high Mach number), with an increase in the Mach number, ion reflection becomes crucial for ion heating (Chodura 1975; Sckopke *et al.* 1983; Burgess, Wilkinson & Schwartz 1989; Sckopke *et al.* 1990; Zimbardo 2011; Gedalin 2019*c*; Madanian *et al.* 2021). The reflected ions are responsible for the foot formation (Woods 1969, 1971) and were thought being responsible for the overshoot increase (Mellott & Livesey 1987). Ion reflection has been approximately described as specular for quite a while Woods (1969, 1971). The specular reflection approximation assumes that ions are reflected by the cross-shock potential without entering the shock. In the upstream region the uniform magnetic field and the motional electric field ensure the drift of ions with a velocity V_u along the shock. This description refers to the normal incidence frame (NIF). The NIF is the reference frame in which the shock is static and the upstream plasma flow $(V_u, 0, 0)$ is along the shock normal. Inside the shock transition layer, the magnetic field increases and the magnetic force is no longer balanced by the electric force due to the motional electric field. The specular reflection approximation ignores the effect of this magnetic force on the ion motion. It was found that specular reflection requires extremely high cross-shock potentials (Wilkinson & Schwartz 1990). It has been recently shown (Balikhin & Gedalin 2022) that the widely used expression for the shock foot width, based on the specular reflection approximation (Gosling & Robson 1985), may overestimate the width by a factor of two. The significance of the magnetic field is the primary distinction between the processes of specular and non-specular reflection (Gedalin 1996). The reflection process of an ion depends on the initial values of the velocity of an ion (Gedalin *et al.* 2020). The process of non-specular reflection determines the velocities of the reflected ions with which they start to gyrate in the upstream region ahead of the ramp. In quasi-perpendicular shocks most of these ions return to the shock and cross it again, constituting the population of reflected–transmitted ions. Knowledge of the distribution of the reflected ions in the upstream region and of the reflected–transmitted ions is essential for understanding of the ion heating, the effect of ions on the shock structure and possible instabilities in the foot region (Burgess *et al.* 2016). So far non-specular reflection has been studied within simulations (see, e.g. Burgess *et al.* 1989; Burgess & Scholer 2007; Burgess

et al. 2016) or test particle analyses (Gedalin 1996, 2016). These are able to provide the detailed information on the reflection process and the distributions, but only in numerical form. Deeper understanding of the role of electrostatic and magnetic forces in the ion reflection requires analytical treatment. In the present paper, we propose an approximate analytical approach which allows us to determine the non-specular ion velocities and the distributions of the reflected ions ahead of the ramp and during the second crossing of the shock.

2. Non-specular reflection inside the shock front

In this section we consider the ion reflection process, that is, the deceleration of an ion inside the ramp and overshoot region (up to the overshoot maximum) and return to the upstream region. The forthcoming analysis is in NIF. The shock normal is along the x-axis. The upstream and downstream magnetic fields are in the x–z plane. In what follows, it is convenient to use the dimensionless variables. The magnetic field is normalized on the upstream magnetic field magnitude B_u, the velocity is normalized on the upstream NIF plasma velocity V_u, the electric field is normalized on $V_u B_u/c$, the spatial coordinates are normalized on the upstream ion convective gyroradius V_u/Ω_u and the time is normalized on the inverse upstream gyrofrequency Ω_u^{-1}, where $\Omega_u = eB_u/mc$, m being the proton mass, e and c are the proton charge and speed of light respectively . The shock is assumed planar and stationary. The normalized fields are

$$B_x = \cos\theta_{Bn}, \quad B_y = 0, \quad B_z = \sin\theta_{Bn} \tag{2.1a–c}$$

$$E_x = 0, \quad E_y = \sin\theta_{Bn}, \quad E_z = 0 \tag{2.2a–c}$$

in the uniform upstream region ahead of the ramp, $x < 0$, and

$$B_x = \cos\theta_{Bn}, \quad B_y = B_y(x), \quad B_z = B_z(x) \tag{2.3a–c}$$

$$E_x = E_x(x) \quad E_y = \sin\theta_{Bn}, \quad E_z = 0 \tag{2.4a–c}$$

in the ramp-overshoot region $x > 0$. Here E is the normalised cross-shock electric field. In this section we are treating the ion motion for $x > 0$. The equations of motion (in the normalized form) read

$$\frac{\mathrm{d}v_x}{\mathrm{d}t} = E_x + v_y B_z - v_z B_y, \tag{2.5}$$

$$\frac{\mathrm{d}v_y}{\mathrm{d}t} = \sin\theta_{Bn} + v_z \cos\theta_{Bn} - v_x B_z, \tag{2.6}$$

$$\frac{\mathrm{d}v_z}{\mathrm{d}t} = v_x B_y - v_y \cos\theta_{Bn}, \tag{2.7}$$

$$\frac{\mathrm{d}x}{\mathrm{d}t} = v_x. \tag{2.8}$$

We are interested in the reflected ions. An ion is reflected if, at some point $x_r < L$ inside the ramp-overshoot region, the velocity along the shock normal drops to zero, $v_x(x_r) = 0$. Here, L denotes the width of the region. Up to the reflection point $x = x_r$ the velocity v_x does not change sign, so that it is possible to replace $(\mathrm{d}/\mathrm{d}t) = v_x(\mathrm{d}/\mathrm{d}x)$ and integrate

$$v_x^2 - v_{x0}^2 = -s(x) + 2\int_0^x (v_y B_z - v_z B_y)\,\mathrm{d}x', \tag{2.9}$$

$$v_y = v_{y0} + \int_0^x \left(\frac{\sin\theta_{Bn} + v_z \cos\theta_{Bn}}{v_x} - B_z\right)\mathrm{d}x', \tag{2.10}$$

$$v_z = v_{z0} + \int_0^x \left(B_y - \frac{v_y \cos\theta_{Bn}}{v_x}\right) dx', \tag{2.11}$$

where

$$s(x) = -2\int_0^x E_x(x')\, dx', \tag{2.12}$$

is the NIF cross-shock potential which is normalized on $mV_u^2/2$. The electric field inside the ramp is highly inhomogeneous. It is determined by ion–electron decoupling, and depends on the electron temperature and peculiarities of the ion dynamics. The dependence $s(x)$ is built to be self-consistently affected by the particle motion and also affects this motion. At present, there is no good knowledge of the fine structure of the shock front. In our calculations only the total potential drop is of importance and not the details of the functional dependence $s(x)$. For the incident ions both initial v_y and v_z are of the order of the upstream thermal speed $v_T = \sqrt{\beta/2}/M$, normalized on V_u. Here, $M = V_u/v_A$ is the Alfvénic Mach number, the Alfvén speed is $v_A = B_u/\sqrt{4\pi n_u m}$, n_u is the upstream ion number density, $\beta = 8\pi n_u T_u/B_u^2$ is the ratio of the upstream ion kinetic pressure to the upstream magnetic pressure and T_u is the upstream ion temperature. For $\beta \lesssim 1$ and $M \sim 5$ one has $v_T \sim 0.1 \ll 1$. Thus, both initial v_{y0} and v_{z0} are small. The non-coplanar component B_y peaks inside the ramp and $\int B_y\, dx$ is typically much smaller than $\int B_z\, dx$ (Goodrich & Scudder 1984; Jones & Ellison 1987), so that we approximate (2.9) as follows:

$$v_x^2 - v_{x0}^2 = -s_{\text{eff}}(x), \tag{2.13}$$

$$s_{\text{eff}}(x) = s(x) - v_{y0}A(x), \tag{2.14}$$

$$A(x) = 2\int_0^x B_z(x')\, dx'. \tag{2.15}$$

Note that the effective cross-shock potential, defined by (2.14), depends on x only for a given initial v_{y0}. The integral $A(x)$ monotonically increases. The electrostatic cross-shock potential is expected to increase with the magnetic field, up to the overshoot maximum (Goodrich & Scudder 1984; Jones & Ellison 1987; Schwartz *et al.* 1988). An ion is reflected if $v_x = 0$ at some position inside the ramp-overshoot region. Let the width of the ramp-overshoot region (up to the overshoot maximum approximately) be L. Without the magnetic contribution, all ions with $v_{x0}^2 < s(L)$ would be reflected. For a typical $s(L) = 0.5$ (Morse 1973; Formisano 1982; Schwartz *et al.* 1988; Dimmock *et al.* 2012; Hanson *et al.* 2019) one has $v_{x0} \lesssim 1 - 3v_T$, which is in the tail of the Maxwellian distribution function (see, e.g. Sckopke *et al.* 1983)

$$f_u(v_x, v_y) = \frac{n_u}{(2\pi)^{3/2}v_T^3} \exp\left(-\frac{(v_x-1)^2}{2v_T^2} - \frac{v_y^2}{2v_T^2}\right), \tag{2.16}$$

so that the number of reflected ions would be small. For $v_{y0} > 0$, the effective potential reduces relative to the electrostatic cross-shock potential, so that these velocities are unfavourable for ion reflection. For v_{y0}, the effective potential exceeds the electrostatic potential, thus enhancing the ion reflection. Therefore, the ions whose initial velocity satisfies the condition

$$v_{x0}^2 < s_{\text{eff}}(L) \tag{2.17}$$

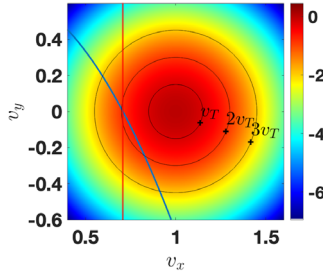$$s_{\text{eff}}(L) = s(L) - v_{y0}A(L), \tag{2.18}$$

FIGURE 1. Initial Maxwellian distribution of ions with $v_T = 0.15$. The ions to the left of the red line would be reflected if the reflection process were specular. The ions to the left of the blue line are non-specularly reflected. The contours for $|\boldsymbol{v} - \boldsymbol{V}_u| = v_T$, $2v_T$ and $3v_T$ are shown.

would be reflected, while others will cross the shock without stopping inside.

Figure 1 shows the part of the velocity space of the incident Maxwellian distribution, corresponding to the reflected ions for specular and non-specular reflection, for $v_T = 0.15$, $s = 0.5$ and $A = 0.75$. The latter is estimated as $\sim B_{\max}L$, where $L \sim \sqrt{1-s}/B_{\max}$ (Gedalin *et al.* 2022). If the reflection were specular, $\approx 2.5\,\%$ of the total number of ions would be reflected. The non-specular reflection results in $\approx 4\,\%$ of reflected ions. For $v_T = 0.1$, the percentage of the reflected ions is $0.16\,\%$ and $0.43\,\%$, respectively. For $v_T = 0.2$ we have $7\,\%$ and $9\,\%$, respectively.

After the ion passes through the point of reflection, it comes back to the beginning of the ramp. In the same approximation as above, the ion would have $v_{x1} = -v_{x0}$, $v_{y1} = v_{y0}$ and $v_{z1} = v_{z0}$ when it enters the upstream region again. Note that, in our approximation, the number of reflected ions and their velocities $\boldsymbol{v}_1$ do not depend on the shock angle θ_{Bn}.

3. Gyration of the reflected ions in the upstream region

The equations of motion of the reflected ion in the upstream region are

$$\frac{dv_x}{dt} = v_y \sin\theta_{Bn} \tag{3.1}$$

$$\frac{dv_y}{dt} = \sin\theta_{Bn} + v_z \cos\theta_{Bn} - v_x \sin\theta_{Bn} \tag{3.2}$$

$$\frac{dv_z}{dt} = -v_y \cos\theta_{Bn} \tag{3.3}$$

$$\frac{dx}{dt} = v_x, \tag{3.4}$$

with the initial conditions $\boldsymbol{v} = \boldsymbol{v}_1$ and $x = 0$ at $t = 0$. The solution of the equations of motion with the specified initial conditions is

$$\begin{aligned} x = {} & (v_{x1}\cos^2\theta_{Bn} + v_{z1}\sin\theta_{Bn}\cos\theta_{Bn} + \sin^2\theta_{Bn})t \\ & + (v_{x1}\sin\theta_{Bn} - v_{z1}\cos\theta_{Bn} - \sin\theta_{Bn})\sin\theta_{Bn}\sin t \\ & - v_{y1}\sin\theta_{Bn}\cos t + v_{y1}\sin\theta_{Bn} \end{aligned} \tag{3.5}$$

$$\begin{aligned} v_x = {} & (v_{x1}\cos\theta_{Bn} + v_{z1}\sin\theta_{Bn})\cos\theta_{Bn} + \sin^2\theta_{Bn} \\ & + (v_{x1}\sin\theta_{Bn} - v_{z1}\cos\theta_{Bn} - \sin\theta_{Bn})\sin\theta_{Bn}\cos t + v_{y1}\sin\theta_{Bn}\sin t \end{aligned} \tag{3.6}$$

(*a*)   (*b*)
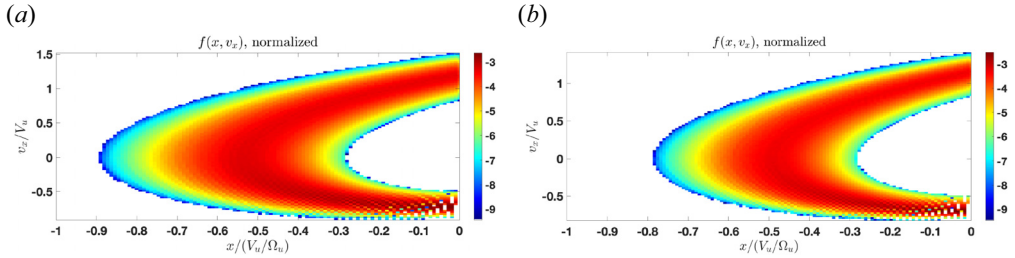

FIGURE 2. Normalized 1-D reduced distribution function $f(x, v_x)$ for non-specularly reflected ions only with $M = 5$, $s = 0.5$, $\beta = 0.5$ and $\theta_{Bn} = 65°$; (*a*) $A = 0.75$, (*b*) $A = 0.375$. Ions which have positive v_x, return to the shock and cross it again.

$$v_y = v_{y1} \cos t_{Bn} - (v_{x1} \sin \theta_{Bn} - v_{z1} \cos \theta_{Bn} - \sin \theta_{Bn}) \sin t \tag{3.7}$$

$$v_z = (v_{x1} \cos \theta_{Bn} + v_{z1} \sin \theta_{Bn}) \sin \theta_{Bn} - \sin \theta_{Bn} \cos \theta_{Bn}$$

$$- (v_{x1} \sin \theta_{Bn} - v_{z1} \cos \theta_{Bn} - \sin \theta_{Bn}) \cos \theta_{Bn} \cos t - v_{y1} \cos \theta_{Bn} \sin t. \tag{3.8}$$

For each $x < 0$, (3.5) has zero, one or two solutions $t(x)$. These solutions, when substituted into (3.6)–(3.8), give $\boldsymbol{v}(x)$. Equation (3.5) cannot be solved analytically. For the further analysis we shall use numerical solution of this equation. For derivation of the reduced distribution function

$$f(x, v_x) = \int f(x, \boldsymbol{v}) \, dv_y \, dv_z \tag{3.9}$$

we have from (3.5)–(3.8) the position and velocities as functions of time for 10^6 ions initially uniformly distributed in the range $|v_{x0} - 1| < 3v_T$, $|v_{y0}| < 3v_T$, $|v_{z0}| < 3v_T$, after selecting ions which satisfy the conditions $\sqrt{(v_{x0} - 1)^2 + v_{y0}^2 + v_{z0}^2} < 3v_T$ and $v_{x0}^2 < s - Av_{y0}$. For a small time step $\Delta t = 0.02$ the phase space (x, v_x) is sufficiently densely filled.

We catch the reflected ions on a two-dimensional grid in the phase space (x, v_x). Each ion is assigned the weight $|v_{x0}|f_u(\boldsymbol{v}_0)$, where v_{x0} is the x-component of the initial ion velocity, to ensure the conservation of particle flux. These weights for all the particles and all the appearances in the cell $(x, v_x) \to (x + \Delta x, v_x) \to (x + \Delta x, v_x + \Delta v_x) \to (x, v_x + \Delta v_x) \to (x, v_x)$, where the grid cell dimensions are $(\Delta x, \Delta v_x)$, are summed up to form the reduced distribution function. In what follows the basic working set of parameters chosen is follows: $M = 5$, $s = 0.5$, $A = 0.75$, $\beta = 0.5$ and $\theta_{Bn} = 65°$.

Figure 2 shows the one dimensional (1-D) reduced distribution function $f(x, v_x)$ for the basic set (*a*) and for $A = 0.375$ (*b*). For the visualization, the distribution function is normalized so that $\sum_{ij} f(x_i, v_{xj}) = 1$. Here, i and j give the number of cells. For the smaller value of A, the number of reflected ions is smaller by a factor of two, and they move to a smaller distance from the shock. A part of the phase space near the ramp is free of particles, which is usually referred to as an ion phase space hole (Johlander *et al.* 2018).

Figure 3 shows the 1-D reduced distribution function $f(x, v_x)$ for $M = 5$, $s = 0.5$, $\beta = 0.5$, $A = 0.75$ and two smaller angles. For $\theta_{Bn} = 40°$ there is a substantial population of reflected ions which escape further upstream and do not return to the shock, also known as backstreaming ions. Yet, a number of ions do return. They will either cross the shock and proceed further into the downstream region or are reflected once again. Analytical treatment of multiply reflected ions is beyond the scope of the present paper and the capabilities of our approximation.
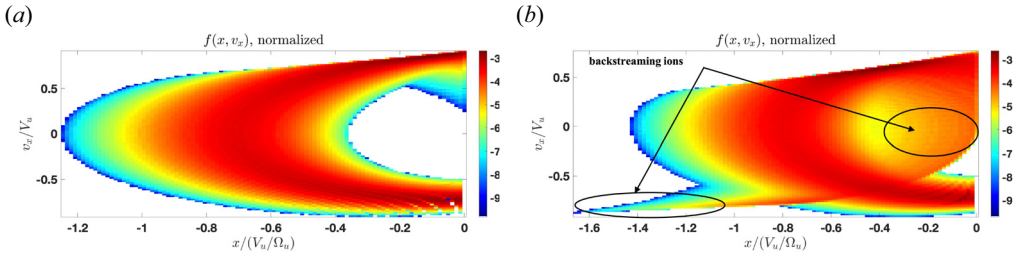
FIGURE 3. Normalized 1-D reduced distribution function $f(x, v_x)$ for non-specularly reflected and backstreaming ions both with $M = 5$, $s = 0.5$, $\beta = 0.5$ and $A = 0.75$; (*a*) $\theta_{Bn} = 45°$, (*b*) $\theta_{Bn} = 40°$. There is a substantial population of backstreaming ions for the smaller angle case. In the right panel, it is clearly visible that ions which have $v_x \approx 0$ mainly do not cross the shock again and escape further upstream and appear as the backstreaming ions.

4. Shock crossing by the reflected–transmitted ions

Upon gyration in the upstream region, in quasi-perpendicular shocks the reflected ions return to the shock and cross it again. Their dynamics inside the shock front is governed by (2.5)–(2.8). For simplicity, we analyse here the perpendicular case $\theta_{Bn} = 90°$, for which $B_x = B_y = 0$. Accordingly, the relevant equations of motion read

$$v_x \frac{\mathrm{d}v_x}{\mathrm{d}x} = E_x + v_y B_z \tag{4.1}$$

$$v_x \frac{\mathrm{d}v_y}{\mathrm{d}x} = 1 - v_x B_z, \tag{4.2}$$

with the initial conditions $v_x = v_{x2}$, $v_y = v_{y2}$ at $x = 0$. The subscript 2 refers to the velocities of the reflected ions at their re-entry to the shock. Integrating the equations, one has

$$v_x^2 = v_{x2}^2 - s + 2 \int_0^x v_y B_z \, \mathrm{d}x', \tag{4.3}$$

$$v_y = v_{y2} + \int_0^x \left(\frac{1}{v_x} - B_z \right) \mathrm{d}x', \tag{4.4}$$

where v_x, v_y, s and B_z are functions of x. Figure 4 shows the reduced distribution function $f(x, v_y)$ for the basic set of parameters. It is seen that the reflected ions re-enter the shock with large positive v_y. Figure 2 shows that the component $v_x > 1$ at the re-entry. Since

$$\left| \int_0^L \left(\frac{1}{v_x} - B_z \right) \mathrm{d}x' \right| < \left| \int_0^L (1 - B_z) \, \mathrm{d}x' \right| < A. \tag{4.5}$$

Therefore, we may approximate $v_y \approx v_{y2}$ and

$$v_{x3}^2 \approx v_{x2}^2 - s + 2A v_{y2}, \tag{4.6}$$

where v_{x3} is the velocity upon crossing the ramp-overshoot region. Figure 5 shows the distribution function $f(x = 0, v_x)$ at the re-entry to the shock (black curve) and $f(x = L, v_x)$ (red curve) of the reflected–transmitted ions upon crossing the ramp-overshoot region. Figure 6 shows the histogram of the ratio v_{x3}/v_{x2}. All reflected–transmitted ions acquire higher v_x upon crossing the shock.
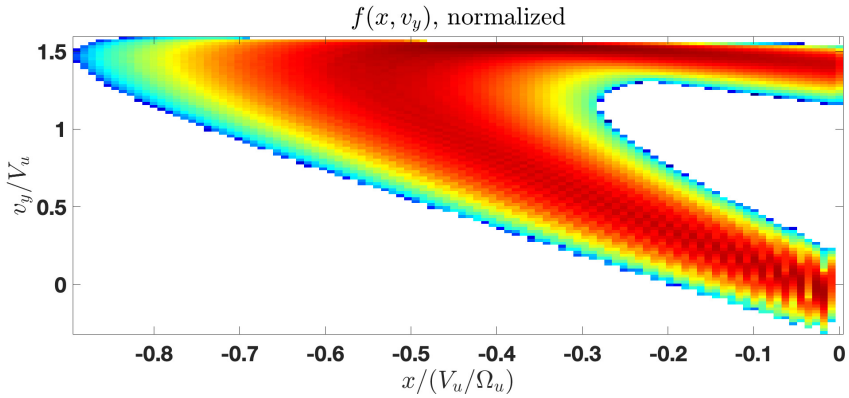
$f(x, v_y)$, normalized

FIGURE 4. Normalized 1-D reduced distribution function $f(x, v_y)$ for non-specularly reflected ions only with $M = 5$, $s = 0.5$, $\beta = 0.5$, $\theta_{Bn} = 65°$ and $A = 0.75$. Ions which have large positive v_y, return to the shock and cross it again.
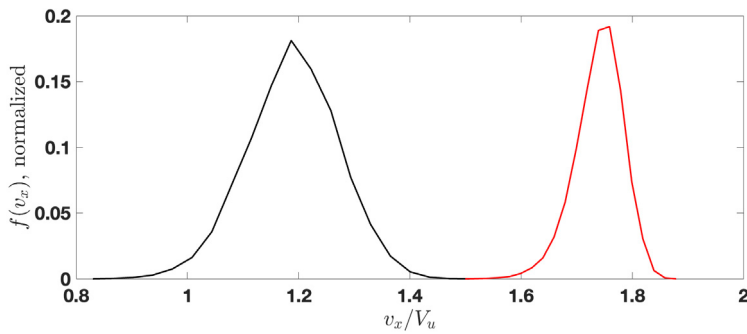

FIGURE 5. The distribution function $f(x = 0, v_x)$ at the re-entry to the shock (black curve) and $f(x = L, v_x)$ (red curve) of the reflected–transmitted ions upon crossing the ramp-overshoot region. The distribution functions are normalized so that $\int f \, \mathrm{d}v_x = 1$.
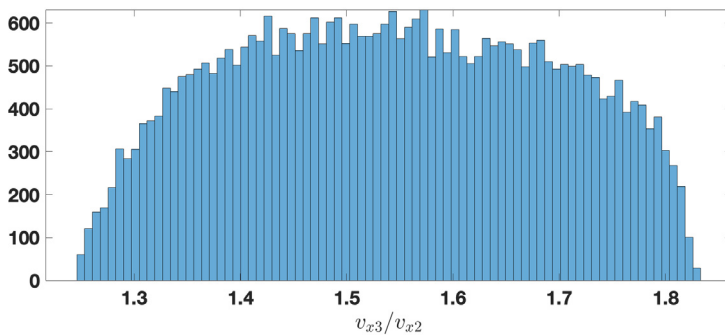

FIGURE 6. The histogram of the ratio v_{x3}/v_{x2}. All reflected–transmitted ions are accelerated across the shock.

The total pressure is related to the reduced distribution function as follows:

$$p_{xx} = m \int v_x^2 f(x, \boldsymbol{v}) \, \mathrm{d}^3 \boldsymbol{v}, \tag{4.7}$$

where p_{xx} is a total pressure including the dynamic and kinetic pressure. In the collisionless system the distribution function is constant along the particle trajectory in the phase space. For the reflected–transmitted ions this means

$$f(x_2, \boldsymbol{v}_2) = f(x_3, \boldsymbol{v}_3). \tag{4.8}$$

The particle flux conservation requires

$$v_{x2} f(x_2, \boldsymbol{v}_2) \, \mathrm{d}^3 \boldsymbol{v}_2 = v_{x3} f(x_3, \boldsymbol{v}_3) \, \mathrm{d}^3 \boldsymbol{v}_3, \tag{4.9}$$

so that

$$p_{3,xx} = \int v_{x3}^2 f(x_3, \boldsymbol{v}_3) \, \mathrm{d}^3 \boldsymbol{v}_3 = \int v_{x3} v_{x2} f(x_2, \boldsymbol{v}_2) \, \mathrm{d}^3 \boldsymbol{v}_2 > p_{2,xx}. \tag{4.10}$$

The immediate consequence of the increase of v_x across the shock is that the contribution of the reflected–transmitted ions to p_{xx} of all ions increases at the shock crossing. The momentum conservation in the planar stationary shock (pressure balance equation) reads

$$p_{\mathrm{tot},xx} + \frac{B^2}{8\pi} = \mathrm{const.}, \tag{4.11}$$

which means that a decrease in the plasma pressure should be balanced by the corresponding increase of the magnetic pressure. The ion pressure $p_{i,xx}$ inside the ramp-overshoot region is the sum of the decreasing pressure of the directly transmitted ions and the increasing pressure of the reflected–transmitted ions. The deceleration of the directly transmitted ions is responsible for the magnetic field increase, that is, the overshoot growth, while the reflected–transmitted ions contribute to limit the maximum of the overshoot.

5. Conclusions

We proposed, for the first time, an approximate analytical description of the non-specular ion reflection in the shock front, taking into account both the electrostatic deceleration and the magnetic deflection. It is shown that, in the reflection condition, the electrostatic cross-shock potential should be replaced with an effective potential proportional to the magnetic field, integrated over the reflection region, and to the initial ion velocity in the direction perpendicular to the coplanarity plane. The magnetic contribution substantially increases the number of reflected particles. The velocity distribution of the reflected ions differs significantly from that obtained within the specular reflection approximation. The reflected particles further gyrate in the upstream region and return to the shock. Using the analytical solution of the equations of ion motion in the uniform upstream region and the initial velocity space derived at the previous step, we numerically constructed the reduced distribution function of reflected ions ahead of the ramp. We have explicitly shown that a smaller magnetic contribution results in a reduction of the number of reflected particles and smaller turning distances of these reflected ions. For smaller angles, in the quasi-parallel range but still close to the boundary between the quasi-parallel and quasi-perpendicular regimes, a population of reflected ions returning to the shock coexists with a population of ions which escape further upstream (backstreaming

ions). We determined the velocities of the ions at the re-entry to the shock. The component v_x significantly exceeds the upstream plasma speed, the component $v_y \sim 1.5V_u$ at this point. We have developed an analytical approximation to establish a relation between the v_x of the reflected–transmitted ions at their re-entry into the shock and their v_x upon crossing the ramp-overshoot region. It is shown that v_x increases for all these ions, that is, they are accelerated by the magnetic force despite electrostatic deceleration. Therefore, the total pressure p_{xx} of these ions increases across the shock. Thus, they contribute towards limiting the overshoot growth due to the deceleration of the directly transmitted ions.

The proposed approach is the first analytical treatment of the non-specular ion reflection and its implications. This is the lowest-order approximation and lays out a basis for more sophisticated analyses.

Acknowledgements

Funding

Declaration of interests

The authors report no conflict of interest.

REFERENCES

BALE, S.D., BALIKHIN, M.A., HORBURY, T.S., KRASNOSELSKIKH, V.V., KUCHAREK, H., MÖBIUS, E., WALKER, S.N., BALOGH, A., BURGESS, D., LEMBÈGE, B., *et al.* 2005 Quasi-perpendicular shock structure and processes. *Space Sci. Rev*. **118** (1), 161–203.

BALIKHIN, M.A., ZHANG, T.L., GEDALIN, M., GANUSHKINA, N.Y. & POPE, S.A. 2008 Venus express observes a new type of shock with pure kinematic relaxation. *Geophys. Res. Lett*. **35** (1).

BALIKHIN, M. & GEDALIN, M. 2022 Collisionless shocks in the heliosphere: foot width revisited. *Astrophys. J*. **925** (1), 90.

BELL, A.R. 1978 The acceleration of cosmic rays in shock fronts–I. *Mon. Not. R. Astron. Soc*. **182** (2), 147–156.

BURGESS, D., HELLINGER, P., GINGELL, I. & TRÁVNÍČEK, P.M. 2016 Microstructure in two- and three-dimensional hybrid simulations of perpendicular collisionless shocks. *J. Plasma Phys*. **82** (4), 905820401.

BURGESS, D., LUCEK, E.A., SCHOLER, M., BALE, S.D., BALIKHIN, M.A., BALOGH, A., HORBURY, T.S., KRASNOSELSKIKH, V.V., KUCHAREK, H., LEMBÈGE, B., *et al.* 2005 Quasi-parallel shock structure and processes. *Space Sci. Rev*. **118** (1), 205–222.

BURGESS, D. & SCHOLER, M. 2007 Shock front instability associated with reflected ions at the perpendicular shock. *Phys. Plasmas* **14** (1), 012108.

BURGESS, D., WILKINSON, W.P. & SCHWARTZ, S.J. 1989 Ion distributions and thermalization at perpendicular and quasi-perpendicular supercritical collisionless shocks. *J. Geophys. Res.: Space* **94** (A7), 8783–8792.

BYKOV, A.M., VAZZA, F., KROPOTINA, J.A., LEVENFISH, K.P. & PAERELS, F.B.S. 2019 Shocks and non-thermal particles in clusters of galaxies. *Space Sci. Rev*. **215** (1), 1–35.

CHODURA, R. 1975 A hybrid fluid-particle model of ion heating in high-Mach-number shock waves. *Nucl. Fusion* **15** (1), 55.

DE HOFFMANN, F. & TELLER, E. 1950 Magneto-hydrodynamic shocks. *Phys. Rev*. **80** (4), 692.

DIMMOCK, A.P., BALIKHIN, M.A., KRASNOSELSKIKH, V.V., WALKER, S.N., BALE, S.D. & HOBARA, Y. 2012 A statistical study of the cross-shock electric potential at low Mach number, quasi-perpendicular bow shock crossings using cluster data. *J. Geophys. Res*. **117** (A), 02210.

FARRIS, M.H., RUSSELL, C.T. & THOMSEN, M.F. 1993 Magnetic structure of the low beta, quasi-perpendicular shock. *J. Geophys. Res.: Space* **98** (A9), 15285–15294.

FORMISANO, V. 1982 Measurement of the potential drop across the Earth's collisionless bow shock. *Geophys. Res. Lett.* **9**, 1033.

GEDALIN, M. 1996 Ion reflection at the shock front revisited. *J. Geophys. Res.: Space* **101** (A3), 4871–4878.

GEDALIN, M. 1997 Ion heating in oblique low-Mach number shocks. *Geophys. Res. Lett.* **24** (2), 2511–2514.

GEDALIN, M. 2016 Transmitted, reflected, quasi-reflected, and multiply reflected ions in low-Mach number shocks. *J. Geophys. Res.: Space* **121** (11), 10–754.

GEDALIN, M. 2019a Kinematic collisionless relaxation and time dependence of supercritical shocks with alpha particles. *Astrophys. J.* **880** (2), 140.

GEDALIN, M. 2019b Kinematic collisionless relaxation of ions in supercritical shocks. *Front. Phys.* **7**, 692.

GEDALIN, M. 2019c Kinematic collisionless relaxation of ions in supercritical shocks. *Front. Phys.* **7**, 114.

GEDALIN, M. 2021 Shock heating of directly transmitted ions. *Astrophys. J.* **912** (2), 82.

GEDALIN, M., DIMMOCK, A.P., RUSSELL, C.T., POGORELOV, N.V. & ROYTERSHTEYN, V. 2023 Role of the overshoot in the shock self-organization. *J. Plasma Phys.* **89** (2), 905890201.

GEDALIN, M., FRIEDMAN, Y. & BALIKHIN, M. 2015 Collisionless relaxation of downstream ion distributions in low-Mach number shocks. *Phys. Plasmas* **22**, 072301.

GEDALIN, M., GOLBRAIKH, E., RUSSELL, C.T. & DIMMOCK, A.P. 2022 Theory helps observations: determination of the shock Mach number and scales from magnetic measurements. *Front. Phys.* **10**, 11.

GEDALIN, M., ZHOU, X., RUSSELL, C.T. & ANGELOPOULOS, V. 2020 Overshoot dependence on the cross-shock potential. In *Annales Geophysicae* (ed. P. Wurz), vol. 38, pp. 17–26. Copernicus GmbH.

GOODRICH, C.C. & SCUDDER, J.D. 1984 The adiabatic energy change of plasma electrons and the frame dependence of the cross-shock potential at collisionless magnetosonic shock waves. *J. Geophys. Res.: Space* **89** (A8), 6654–6662.

GOODRICH, K.A., ERGUN, R., SCHWARTZ, S.J., WILSON, L.B. III, JOHLANDER, A., NEWMAN, D., WILDER, F.D., HOLMES, J., BURCH, J., TORBERT, R., *et al.* 2019 Impulsively reflected ions: a plausible mechanism for ion acoustic wave growth in collisionless shocks. *J. Geophys. Res.: Space* **124** (3), 1855–1865.

GOSLING, J.T. & ROBSON, A.E. 1985 Ion Reflection, Gyration, and Dissipation at Supercritical Shocks. *Collisionless Shocks in the Heliosphere: Reviews of Current Research*, vol. 35, pp. 141–152, Wiley Online Library.

GOSLING, J.T., THOMSEN, M.F., BAME, S.J., FELDMAN, W.C., PASCHMANN, G. & SCKOPKE, N. 1982 Evidence for specularly reflected ions upstream from the quasi-parallel bow shock. *Geophys. Res. Lett.* **9** (12), 1333–1336.

HANSON, E.L.M., AGAPITOV, O.V., MOZER, F.S., KRASNOSELSKIKH, V., BALE, S.D., AVANOV, L., KHOTYAINTSEV, Y. & GILES, B. 2019 Cross-shock potential in rippled versus planar quasi-perpendicular shocks observed by MMS. *Geophys. Res. Lett.* **46** (5), 2381–2389.

JOHLANDER, A., VAIVADS, A., KHOTYAINTSEV, Y.V., GINGELL, I., SCHWARTZ, S.J., GILES, B.L., TORBERT, R.B. & RUSSELL, C.T. 2018 Shock ripples observed by the MMS spacecraft: ion reflection and dispersive properties. *Plasma Phys. Control. Fusion* **60** (12), 125006.

JONES, F.C. & ELLISON, D.C. 1987 Noncoplanar magnetic fields, shock potentials, and ion deflection. *J. Geophys. Res.* **92** (A10), 11205.

KENNEL, C.F., EDMISTON, J.P. & HADA, T. 1985 *A Quarter Century of Collisionless Shock Research*. Geophysical Monograph Series, vol. 34, pp. 1–36, American Geophysical Union.

LALTI, A., KHOTYAINTSEV, YU.V., DIMMOCK, A.P., JOHLANDER, A., GRAHAM, D.B. & OLSHEVSKY, V. 2022 A database of MMS bow shock crossings compiled using machine learning. *J. Geophys. Res.* **127** (8).

MADANIAN, H., DESAI, M.I., SCHWARTZ, S.J., WILSON, L.B., FUSELIER, S.A., BURCH, J.L., LE CONTEL, O., TURNER, D.L., OGASAWARA, K., BROSIUS, A.L., *et al.* 2021 The dynamics of a high Mach number quasi-perpendicular shock: MMS observations. *Astrophys. J.* **908** (1), 40.

MELLOTT, M.M. & LIVESEY, W.A. 1987 Shock overshoots revisited. *J. Geophys. Res.* **92**, 13661.

MORSE, D.L. 1973 Electrostatic potential rise across perpendicular shocks. *Plasma Phys.* **15** (1), 1262–1264.

OFMAN, L., BALIKHIN, M., RUSSELL, C.T. & GEDALIN, M. 2009 Collisionless relaxation of ion distributions downstream of laminar quasi-perpendicular shocks. *J. Geophys. Res.* **114** (A), 09106.

PERRI, S., BYKOV, A., FAHR, H., FICHTNER, H. & GIACALONE, J. 2022 Recent developments in particle acceleration at shocks: theory and observations. *Space Sci. Rev.* **218** (4), 26.

SAGDEEV, R.Z. & KENNEL, C.F. 1991 Collisionless shock waves. *Sci. Am.* **264** (4), 106–115.

SCHWARTZ, S.J., THOMSEN, M.F., BAME, S.J. & STANSBERRY, J. 1988 Electron heating and the potential jump across fast mode shocks. *J. Geophys. Res.: Space* **93** (A11), 12923–12931.

SCKOPKE, N., PASCHMANN, G., BAME, S.J., GOSLING, J.T. & RUSSELL, C.T. 1983 Evolution of ion distributions across the nearly perpendicular bow shock: specularly and non-specularly reflected-gyrating ions. *J. Geophys. Res.: Space* **88** (A8), 6121–6136.

SCKOPKE, N., PASCHMANN, G., BRINCA, A.L., CARLSON, C.W. & LÜHR, H. 1990 Ion thermalization in quasi-perpendicular shocks involving reflected ions. *J. Geophys. Res.: Space* **95** (A5), 6337–6352.

SCUDDER, J.D., AGGSON, T., AGGSON, T.L., MANGENEY, A., LACOMBE, C. & HARVEY, C.C. 1986 The resolved layer of a collisionless, high beta, supercritical, quasi-perpendicular shock wave. I – Rankine-Hugoniot geometry, currents, and stationarity. *J. Geophys. Res.* **91** (A10), 11019–11052.

STONE, R.G. & TSURUTANI, B.T. 1985 *Collisionless Shocks in the Heliosphere: Reviews of Current Research*. American Geophysical Union.

WILKINSON, W.P. & SCHWARTZ, S.J. 1990 Parametric dependence of the density of specularly reflected ions at quasiperpendicular collisionless shocks. *Planet. Space Sci.* **38** (3), 419–435.

WOODS, L.C. 1969 On the structure of collisionless magneto—plasma shock waves at super—critical Alfvén—Mach numbers. *J. Plasma Phys.* **3** (3), 435–447.

WOODS, L.C. 1971 On double-structured, perpendicular, magneto-plasma shock waves. *Plasma Phys.* **13** (4), 289.

ZIMBARDO, G. 2011 Heavy ion reflection and heating by collisionless shocks in polar solar corona. *Planet. Space Sci.* **59** (7), 468–474.